

# Enhancement of Neurite Outgrowth in Neuronal-Like Cells following Boron Nitride Nanotube-Mediated Stimulation

Gianni Ciofani,<sup>\*,†</sup> Serena Danti,<sup>‡</sup> Delfo D'Alessandro,<sup>\*,§</sup> Leonardo Ricotti,<sup>+</sup> Stefania Moscato,<sup>§</sup> Giovanni Berton,<sup>¶</sup> Andrea Falqui,<sup>¶</sup> Stefano Berrettini,<sup>‡</sup> Mario Petrini,<sup>||</sup> Virgilio Mattoli,<sup>†</sup> and Arianna Menciassi<sup>†,+</sup>

<sup>†</sup>Italian Institute of Technology c/o Scuola Superiore Sant'Anna, Viale Rinaldo Piaggio 34 Pontedera (Pisa), 56025, Italy, <sup>\*</sup>Otology - Cochlear Implant Unit, Department of Neuroscience, University of Pisa, Via Paradisa 2 Pisa, 56124, Italy, <sup>§</sup>Department of Human Morphology & Applied Biology, University of Pisa, Via Roma 55 Pisa, 56126, Italy, <sup>‡</sup>CRIM Lab, Scuola Superiore Sant'Anna, Viale Rinaldo Piaggio 34 Pontedera (Pisa), 56025, Italy, <sup>¶</sup>Italian Institute of Technology, Via Morego 30 Genova, 16163, Italy, and <sup>||</sup>Department of Oncology & Transplants, University of Pisa, Via Roma 55, 56126 Pisa, Italy

**E**lectrical stimulation as an artificial stimulus of neural structures has been widely used in clinical practice and laboratory study. There are multiple strategies reported in the literature and in clinical use that attempt to specifically localize the activation of nervous structures. Efforts have included both invasive and non-invasive approaches, as well as combined technologies.<sup>1,2</sup> Such systems typically involve placement/attachment of an electrode to the target organ/tissue (by surgery or interventional radiology) and a wired connection to the electronic (battery powered) device, which delivers the appropriate electric impulses.<sup>3,4</sup> Despite its technological refinements, the basic configuration of all such systems for electro-stimulation therapies has two inherent disadvantages: (i) contact problems at the electrode/tissue interface and (ii) complications due to the implantation of the stimulator. In this paper we present a new technology based on indirect, noninvasive electrical stimulation mediated by piezoelectric nanoparticles (boron nitride nanotubes, BNNTs<sup>5</sup>) and ultrasounds; in particular, our preliminary results demonstrated that this method could successfully stimulate neuronal-like cell cultures *in vitro*.

A boron nitride nanotube (BNNT) is the structural analogue of a carbon nanotube: alternating B and N atoms entirely substitute for C atoms in a graphitic-like sheet with almost no changes in atomic spacing. In spite of this structural similarity with carbon nanotubes (CNTs), BNNTs own superior mechanical, chemical, and electrical properties.<sup>6</sup> In the last years several examples of

**ABSTRACT** In this paper, we propose an absolutely innovative technique for the electrical stimulation of cells, based on piezoelectric nanoparticles. Ultrasounds are used to impart mechanical stress to boron nitride nanotubes incubated with neuronal-like PC12 cells. By virtue of their piezoelectric properties, these nanotubes can polarize and convey electrical stimuli to the cells. PC12 stimulated with the present method exhibit neurite sprout 30% greater than the control cultures after 9 days of treatment.

**KEYWORDS:** boron nitride nanotubes · PC12 cells · piezoelectric stimulation · neuronal regeneration

CNT exploitation in biotechnology have been proposed,<sup>7</sup> while the biomedical applications of BNNTs have remained largely unexplored.<sup>8</sup> The first studies about BNNT–cell interactions have been performed by the authors in refs 9 and 10. Recent investigations have confirmed that BNNTs also have excellent piezoelectric properties. *Ab initio* calculations of the spontaneous polarization and piezoelectric properties of BNNTs have demonstrated that they function as excellent piezoelectric systems with response values greater than those of piezoelectric polymers, and comparable to those exhibited by wurtzite semiconductors.<sup>11</sup> In addition, BNNT bending forces have been measured directly inside high-resolution transmission electron microscopy, and real-time video-recording of their elastic kinking deformation has confirmed their marked flexibility.<sup>12</sup> Recently, Bai et al. have experimentally verified a deformation-driven electrical transport and the first evidence of a piezoelectric behavior in multiwalled BNNTs.<sup>13</sup> The insulating character of an individual BNNT can be modified by tube squeezing between two gold contacts inside a TEM. A considerable

\*Address correspondence to g.ciofani@sssup.it.

Received for review November 17, 2009 and accepted September 27, 2010.

Published online October 6, 2010. 10.1021/nn101985a

© 2010 American Chemical Society

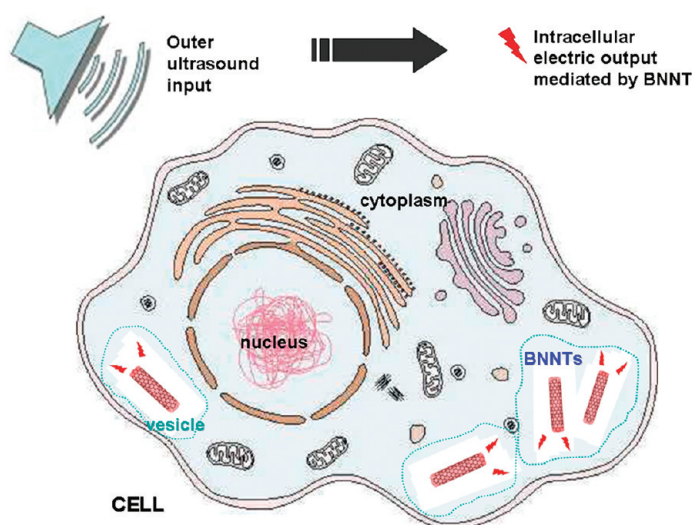


**Figure 1.** “Wireless” electrical stimulation of cells: every cell internalizing piezoelectric nanoparticles (e.g., BNNTs) is subject to inner electric stimulation as a consequence of external ultrasound irradiation.

current of several tens of nA is then able to flow through the tube. Such transport has been confirmed to be reversible, and disappears almost completely after tube reloading. These observations underpin the very high potential of BNNTs as efficient novel nanoscale transducers.

The aim of our study is the exploitation of BNNTs as nanovectors to carry electrical/mechanical signals on demand within a cellular system. Electrical stimuli can be conveyed to a tissue or cell culture after BNNT internalization, using an outer “wireless” mechanical source (i.e., ultrasounds) by virtue of BNNT piezoelectric behavior (Figure 1).

## RESULTS AND DISCUSSION

Stable dispersions of BNNTs were obtained by means of glycol-chitosan (GC) as dispersion agent, on the basis of noncovalent polymeric wrapping. Figure 2 shows a focused ion beam (FIB) micrograph of the BNNTs after preparation: both single nanotubes and small aggregates of nanotubes are visible with dimensions of about 200–600 nm in length and about 50 nm

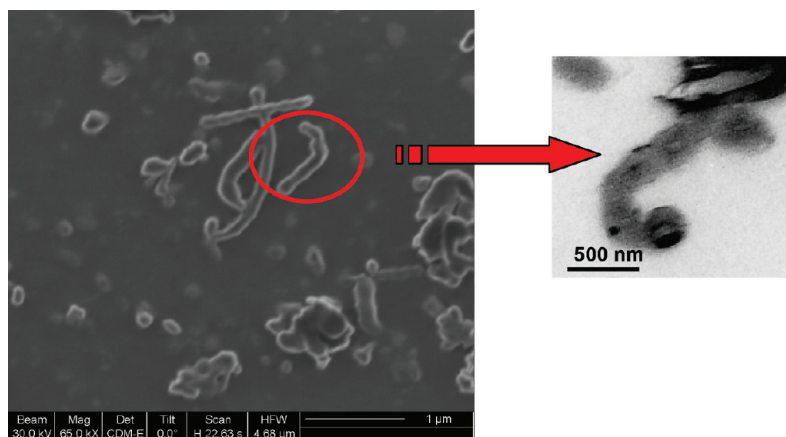


**Figure 2.** FIB and TEM imaging of BNNTs after the dispersion procedure.

in diameter. The inset figure shows an interesting TEM image of a typical “bamboo-like” structure of the BNNTs.

A WST-1 viability assay following cell incubation up to 9 days with BNNT-loaded culture medium (CM) showed nonstatistically significant differences with respect to the controls with BNNT concentrations up to 50  $\mu\text{g}/\text{mL}$  ( $p < 0.05$  for higher concentrations, Figure 3).

Optimal cell viability up to 50  $\mu\text{g}/\text{mL}$  BNNT concentration was confirmed by the LIVE/DEAD viability/cytotoxicity assay (Figure 4), which labels living and dead cells in green and in red, respectively.

Early apoptotic phenomena could be excluded (Figure 4) by investigating changes in the position of phosphatidylserine (PS) in the cell membrane,<sup>14</sup> using annexin V-FITC. The combination of annexin V-FITC with propidium iodide (PI), a red fluorescent DNA-intercalating agent, allowed necrotic (red stained), early apoptotic (green stained), apoptotic (green and red stained), and normal cells (unstained) to be differentiated.

Finally, reactive oxygen species (ROS) production in PC12 cells treated with BNNTs was detected by using the Image-IT Green ROS Detection kit, based on 5-(and-6)-carboxy-2',7'-dichlorodihydrofluorescein diacetate (carboxy- $\text{H}_2\text{DCFDA}$ ), a fluorogenic marker for ROS in viable cells. As shown in Figure 4, BNNTs did not induce significant oxidative stress after 9 days of incubation, even at high concentrations.

Cellular internalization of BNNTs was investigated by TEM analysis (Figure 5). Noncellular electron-dense material with cytoplasmatic vesicle localization, compatible in terms of appearance and size with the BNNTs, was observed. Such observations are consistent with those of Yehia et al.,<sup>15</sup> Raffa et al.,<sup>16</sup> and Tutak et al.<sup>17</sup> performed on different types of mammalian cells exposed to CNT-loaded CM that presented high-resolution TEM images of electron-dense material within intracellular vacuoles.

To definitively prove that the observed intravesicular material is the result of BNNT internalization, images acquired in scanning TEM (STEM) mode (Figure 5a) underwent electron energy loss spectroscopy (EELS), as reported in Figure 5b. This analysis allowed the presence of light chemical elements (namely, B, C, and N) to be detected in the indicated area. Since B and N are the main components of BNNTs and B is not naturally present at the cellular level, the result of EELS confirmed that BNNT uptake by PC12 cells did occur and that such nanotubes are located inside cytoplasmatic vesicles. The C signal stems from organic material, possibly belonging to the BNNT dispersing agent (GC) or to cellular metabolism products. Stimulation of differentiating PC12 cells was carried out as specified in the Meth-

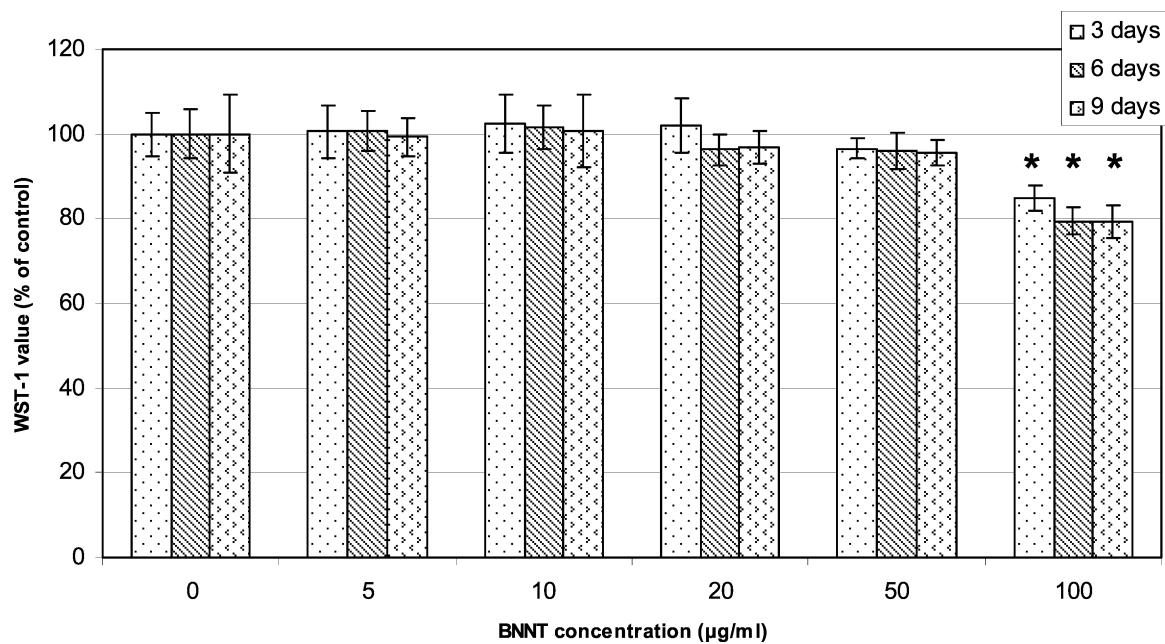


Figure 3. GC-BNNT cytocompatibility results on PC12 cells: WST-1 assay after 3, 6, and 9 days of incubation ( $p < 0.05$ ).

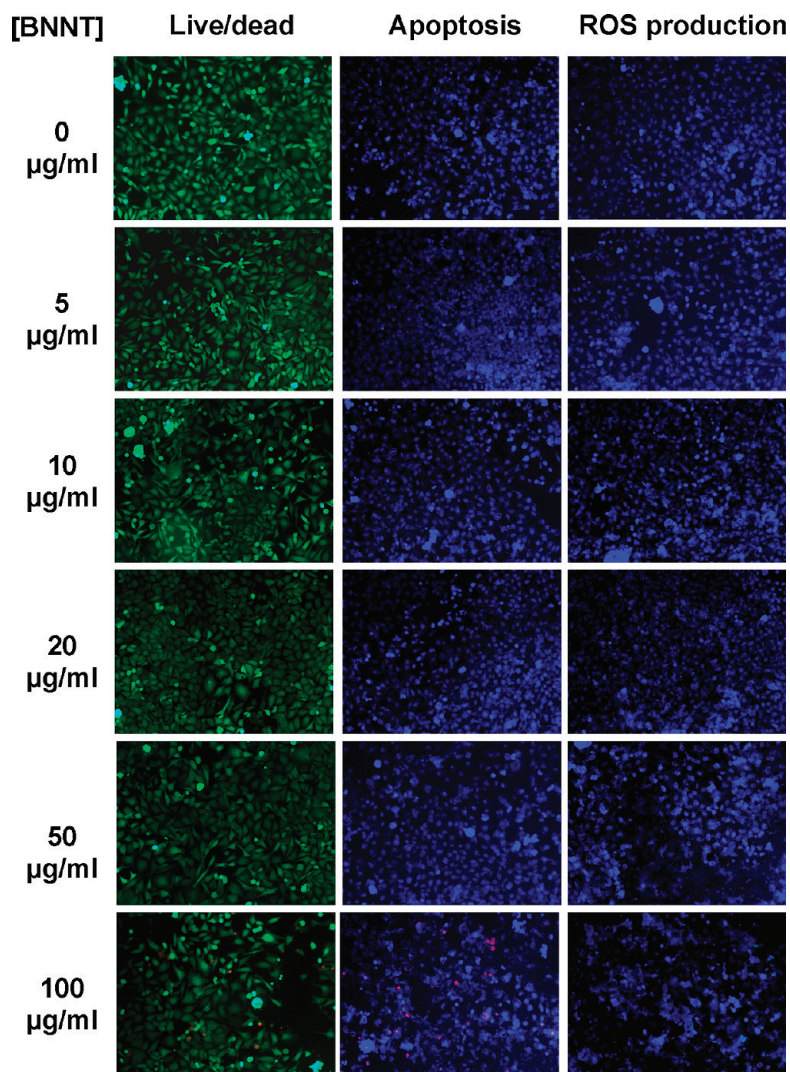


Figure 4. GC-BNNT cytocompatibility results on PC12 cells: live/dead assay, apoptosis, and ROS detection after 9 days of incubation. Magnification 4X.

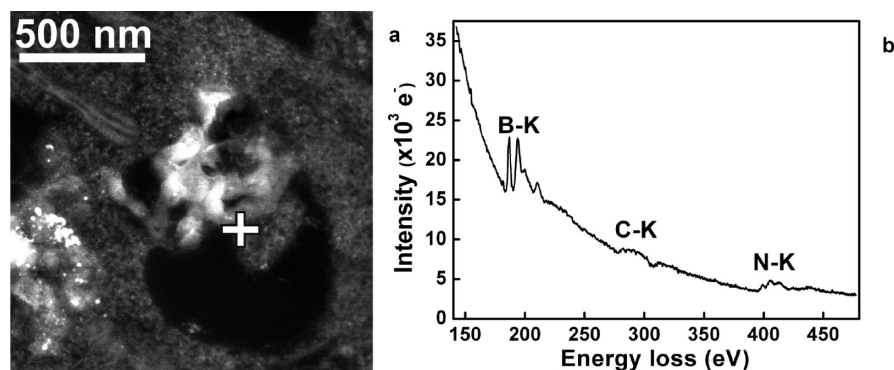


Figure 5. (a) Scanning TEM-high angle annular dark field (STEM-HAADF) image of BNNTs incorporated inside a cytoplasmic vesicle of a PC12 cell. (b) Electron energy loss (EEL) spectrum collected with the electron probe located at the point indicated by a cross in image a and showing the B and N signals coming from the BNNTs. The C signal stems from organic material.

ods section. Up to 9 days of culture, differentiating status (the percentage of differentiated cells in the culture), number of neuronal processes per cell, and neurite length were monitored in cultures incubated with 0, 5, and 10  $\mu\text{g}/\text{mL}$  of BNNTs, both stimulated and nonstimulated with ultrasounds. Figure 6 shows representative micrographs performed on all the groups at the end point.

No significant differences in terms of cellular differentiation could be detected among the groups (Figure 7a): all the cultures reached >95% of differentiation with no differences compared to the control ( $p > 0.05$ ).

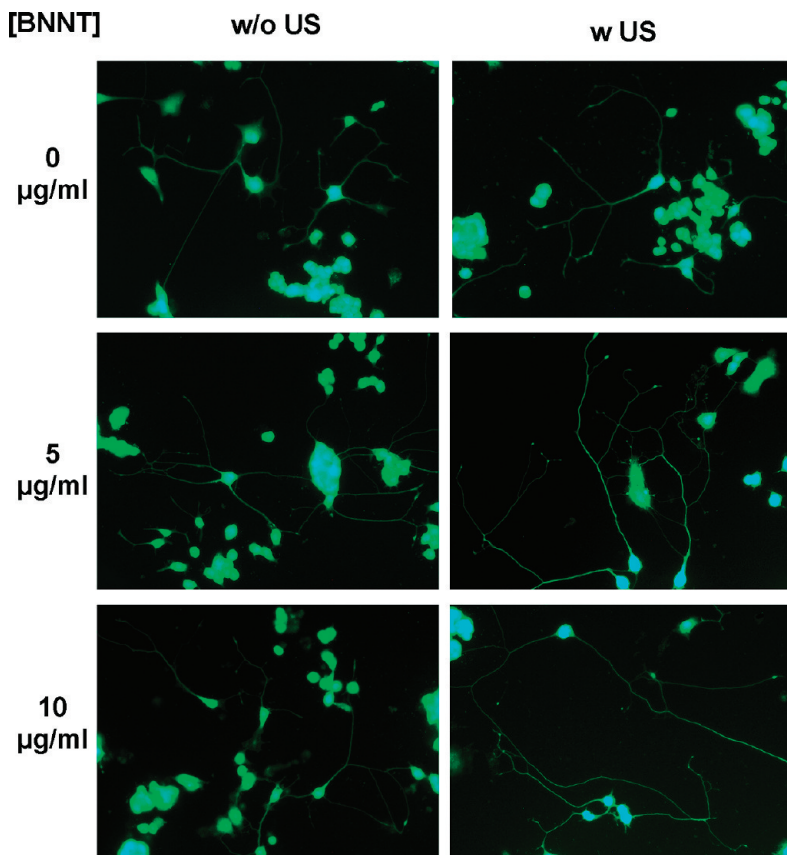


Figure 6. Images of calcein-labeled PC12 cells after 9 days of treatments (with and without BNNT incubation; with and without US stimulation). Magnification 20X.

Interestingly, the number of neuronal processes per differentiated cell became significantly higher in the cultures that underwent both BNNT-incubation and ultrasound stimulation (Figure 7b): on average, about five processes were found in the BNNT-US stimulated cultures with respect to the typical four processes of the control groups ( $p < 0.05$ ). No significant differences were found between the two different BNNT concentrations investigated.

However, a dramatic increment of the developed neurites was the most remarkable outcome ascribable to the combined stimulation. Figure 7c shows the trend of neurite length vs differentiation time. After 72 h of treatment, average neurite length in the BNNT-US groups was clearly higher than that of the control cultures, and this increment rose by about 30% at the end of the 9th day.

To try to clarify the mechanisms underlying the evident effects of the combined stimulation BNNT+US, two tests were carried out with different differentiation inhibitors.

Blockage of the NGF specific receptor TrkA was performed by treating the cells with K252a,<sup>18</sup> as outlined in the Methods section. Cultures (treated with 0 and 10  $\mu\text{g}/\text{mL}$  of BNNTs, with and without ultrasound stimulation) were monitored for 6 days, and the differentiation status was analyzed at the end point (Figure 8a). Differentiation was very low in all the experimental groups (about 5–10%), but increased significantly in the BNNT+US treatment (about 25% of differentiated cells,  $p < 0.05$ ; Figure

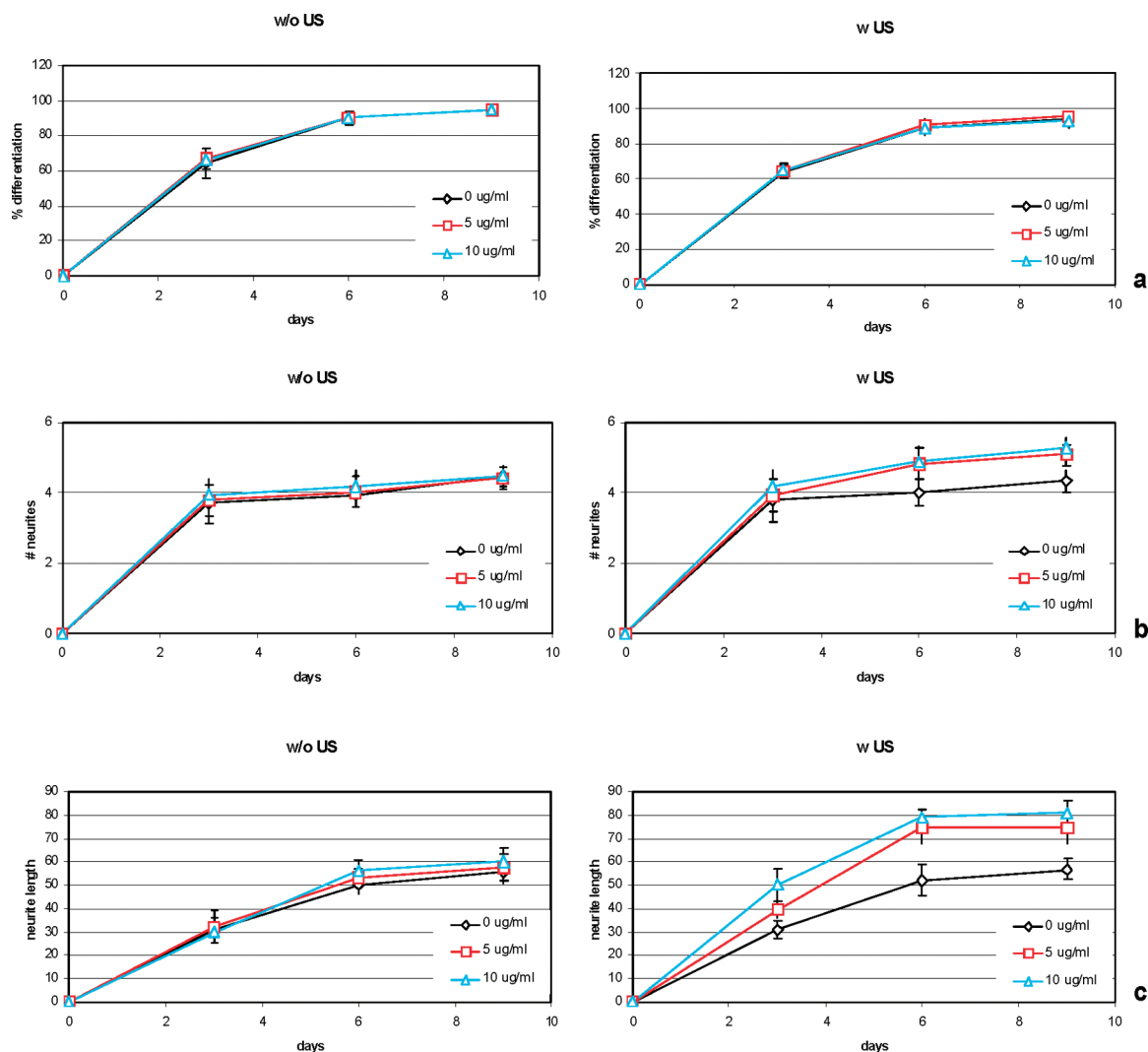


**Figure 7.** Trends of the differentiation (a), number of neurites/cells (b), and neurite lengths (c) during the 9 days of experiments ( $n = 3$ ).

8b, and increased neurite number: Figure 8c). Again, neurite length was significantly higher in the double-stimulated group (about 20  $\mu\text{m}$  with respect to the 8  $\mu\text{m}$  of the other groups,  $p < 0.01$ ; Figure 8d). In any case, we should once again point out that the differentiation state in all the cultures treated with the K252a inhibitor was extremely low, thus demonstrating that the TrkA receptor plays a key role even in the presence of the stimulation with BNNTs and ultrasounds. However, the slight but significant enhancement of differentiation even in the presence of the inhibitor suggests that the stimulation could activate signaling molecules of the differentiation pathway, located downstream to the TrkA receptor. Moreover, the higher differentiative capability of the stimulated samples, observed with or without TrkA inhibitor, could suggest a synergic effect with NGF on the neural differentiation pathway. To evaluate the role of calcium influx, some experiments were repeated with lanthanum ions ( $\text{LaCl}_3$ ), which are known to be nonspecific calcium ion channel blockers.<sup>19</sup> The results are highlighted in Figure 9. In this case, a well-sustained differen-

tiation was observed in all the experimental groups (Figure 9a), with no substantial differences in the differentiation rate (Figure 9b) or in the number of developed neurites (Figure 9c). An increment of neurite length was again highlighted in the case of double stimulation (about 15%,  $p < 0.05$ ; Figure 9d), but was significantly reduced with respect to the results achieved in the absence of  $\text{LaCl}_3$  (Figure 7c).

These results suggest that calcium influx plays a substantial role in the case of BNNT+US stimulation, thus enforcing the hypothesis of indirect electrical stimulation due to the piezoelectric properties of BNNTs, being calcium ions required for the electrically induced development of PC12 neurites.<sup>20</sup>

A final test was conducted on a different neuronal-like cell line, namely SH-SY5Y, which is a neuroblastic subclone of the neuroblastoma cell line SK-N-SH,<sup>21</sup> and is able to differentiate into a functional and morphological neuronal phenotype when treated with retinoic acid,<sup>22</sup> neurotrophic factors, or phorbol esters.<sup>23</sup> Retin-

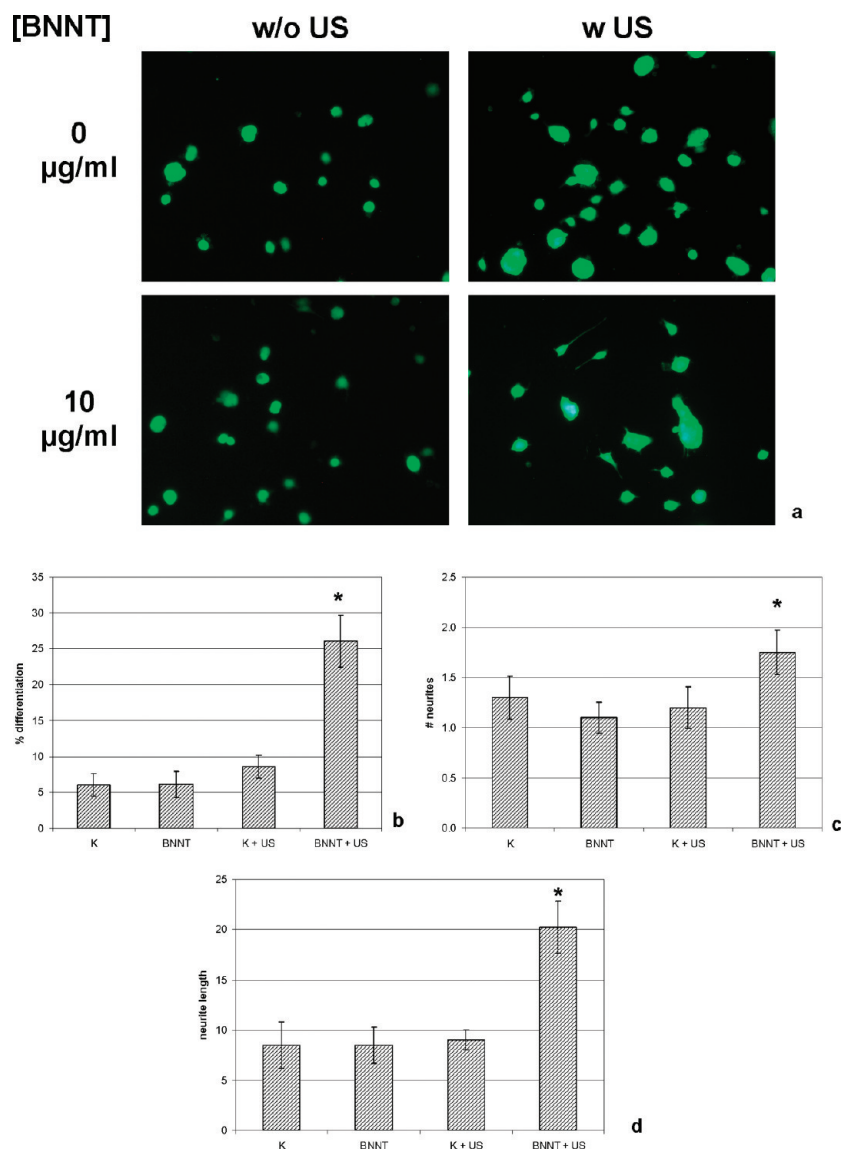


**Figure 8.** Stimulation experiments in the presence of the TrkA inhibitor K252a: images of calcein-labeled PC12 (a), differentiation (b), number of neurites/cells (c), and neurite lengths (d) cells after 6 days of treatments ( $n = 3$ ,  $p < 0.05$ ). Magnification 20X.

oic acid induces differentiation through a pathway that does not involve TrkA, thus allowing to further assess the mechanism of the proposed stimulation. The results are reported in Figure 10. After 6 days of treatment, cultures show a moderate differentiation (about 40% in each experimental group; Figure 10a,b). No differences were observed in the number of developed neurites (Figure 10c) but, once again, a significant increase in neurite length was evidenced on the 6th day of stimulation with ultrasounds in the presence of 10  $\mu\text{g/ml}$  of BNNTs (about 30%,  $p < 0.05$ ; Figure 10d). These data confirm the effects of stimulation on different cell lines, with different differentiation pathways: even if the most important outcomes have been seen in the case of PC12 cells, where TrkA was demonstrated to play a major role also in the stimulation-mediated differentiation, the enhancement of neurite outgrowth

in SH-SY5Y cells demonstrates the efficiency of stimulation also when the TrkA receptor is not involved in the differentiation pathway.<sup>24</sup>

All these results clearly demonstrated an efficient indirect stimulation, opening exciting perspectives in the field of neuronal regeneration.

Several *in vitro* and *in vivo* studies have shown that electrical stimulation plays an important role in neurite extension and in the regeneration of transected nerve ends.<sup>25–27</sup> Electrical charges appear to be focused on the stimulation of axonal regeneration;<sup>28</sup> therefore, many electrical stimulating materials have been evaluated to determine whether they can be used in the development of effective nerve regeneration.<sup>29,30</sup> Although the exact mechanisms by which electrical stimulation favors nerve regeneration have not yet been clearly understood, it is a well-known fact that

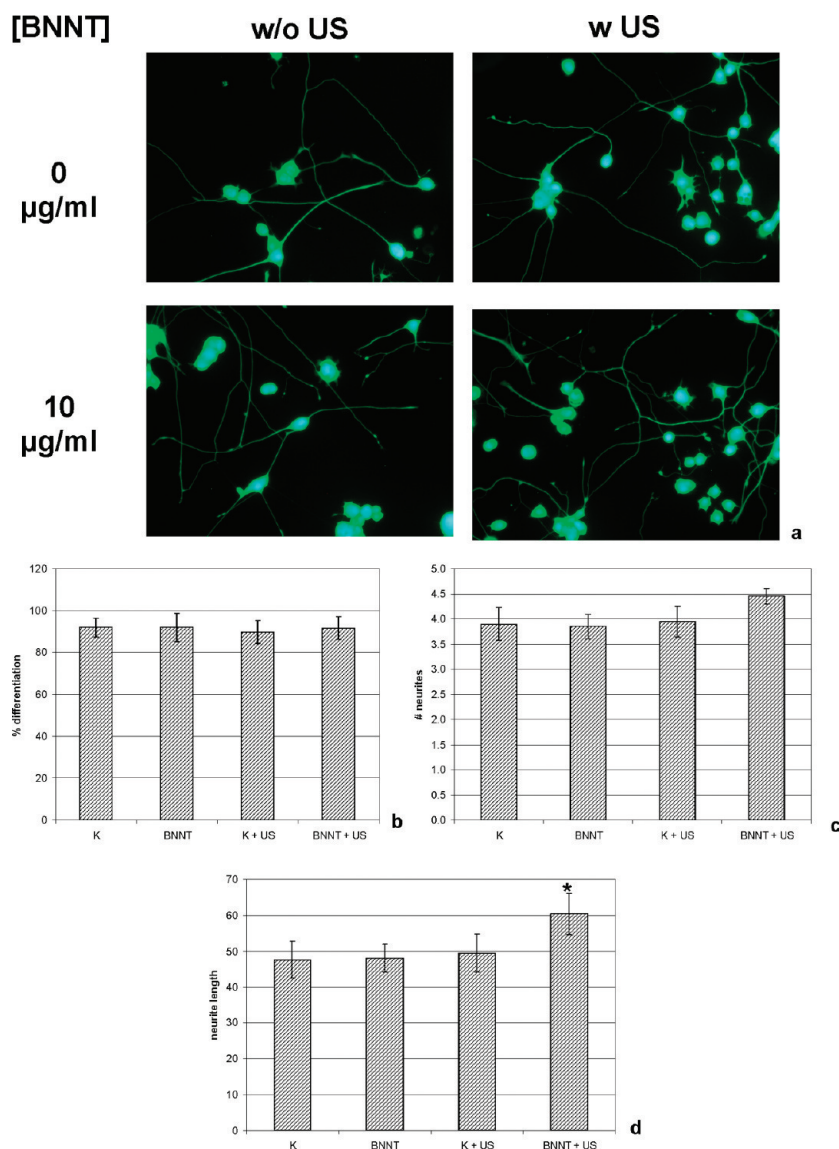


**Figure 9.** Stimulation experiments in the presence of the calcium channels inhibitor  $\text{LaCl}_3$ : images of calcein-labeled PC12 (a), differentiation (b), number of neurites/cells (c), and neurite lengths (d) cells after 6 days of treatments ( $n = 3$ ,  $p < 0.05$ ). Magnification 20X.

electrical stimulation enhances both neurite outgrowth *in vitro*<sup>31,32</sup> and nerve regeneration *in vivo*.<sup>33–36</sup>

Nanotechnology offers several innovative approaches for neuronal stimulation. Carbon nanotubes, for example, have been applied in several areas of nerve tissue engineering to probe and augment cell behavior, to label and track subcellular components, and to study the growth and organization of neural networks. Recent reports have shown that nanotubes can sustain and promote neuronal electrical activity in networks of cultured cells, but the ways in which they affect cellular function are still poorly understood. Using single-cell electrophysiology techniques, electron microscopy analysis, and theoretical modeling, Cellot et al.<sup>37</sup> have demonstrated that nanotubes improve the responsiveness of neurons by forming tight contacts with the cell membranes. Very interestingly, this report shows that

nanotubes can sustain and promote neuronal electrical activity in networks of cultured cells, by favoring electrical shortcuts between the proximal and distal compartments of the neuron.

Recent studies, moreover, have suggested the great potential of high density, carbon nanotube (CNT) coated surfaces as interfacing material with neural systems.<sup>38–46</sup> A study by Shein et al.<sup>47</sup> presents novel carbon nanotube-based electrode arrays composed of cell-alluring CNT islands. These play the double role of anchoring neurons directly and only onto the electrode sites (with no need for chemical treatments) and facilitating high fidelity electrical interfacing-recording and stimulation.

A study by Keefer et al.<sup>48</sup> shows that conventional tungsten and stainless steel wire electrodes can be coated with carbon nanotubes using electrochemical techniques, and that this coating enhances both the re-

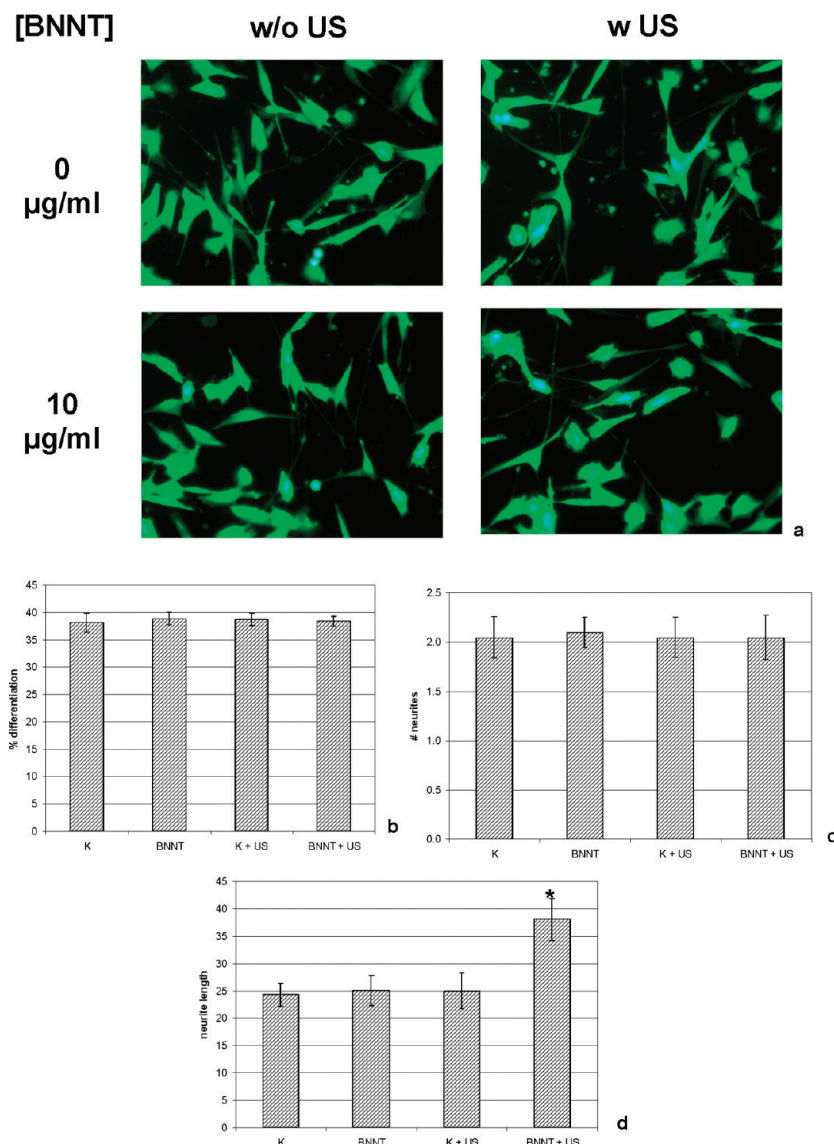


**Figure 10.** Stimulation experiments carried out on human neuroblastoma SH-SY5Y cells: images of calcein-labeled cultures (a), differentiation (b), number of neurites/cells (c), and neurite lengths (d) cells after 6 days of treatments ( $n = 3$ ). Magnification 20X.

cording and electrical stimulation of neurons in culture, rats, and monkeys by decreasing electrode impedance and increasing charge transfer.

Finally, a very recent paper<sup>49</sup> has reported that low concentrations of functionalized CNT, when added with nerve growth factor (NGF), promote the outgrowth of neuronal neurites in dorsal root ganglion (DRG) neurons and in PC12 cells.

Here, we have proposed an innovative solution based on the combination of noninvasive stimulation with US in the presence of piezoelectric nanoparticles incubated with cells, which can elicit the same phenomena derived from a “classical” electric stimulation, i.e., a markedly pronounced outgrowth of neuronal processes in PC12 cultures, but without the need for electrodes in the culture. This was achieved by mechanical stimulation of the BNNTs which, by virtue of their polarizability, are able to

convey electrical stimuli to the cells. Among the already mentioned applications in regenerative medicine, this concept could also be used in life science wherever electrical stimulation is needed, e.g., deep brain stimulation,<sup>50</sup> gastric stimulation for gastroparesis,<sup>51</sup> cardiac pacing for various cardiac arrhythmias,<sup>52</sup> skeletal muscle stimulation in various neuropathies,<sup>53</sup> etc. Of course, before any realistic *in vivo* applications, deep investigations in the BNNT impact on living organisms are mandatory. Biocompatibility, biodistribution, and degradation of these novel nanoparticles have to be tested, owing to the total lack of data in the literature.<sup>54</sup> Active *in vivo* targeting of BNNT toward the site to be treated also should be achieved.

Although extensive and quantitative investigations will be needed after these preliminary results, we are confident in the tremendous impact this technology could have in biological and clinical practices.



## METHODS

**Boron Nitride Nanotubes Preparation.** BNNTs (purchased from the Nano and Ceramic Materials Research Center, Wuhan Institute of Technology, China) were produced using an annealing method from boron containing precursors.<sup>55</sup> Details of the sample provided by the supplier include boron nitride >98.5 wt % and yield >80%.

Glycol chitosan (G-chitosan 81339 from G7753 Sigma) was used for the dispersion and stabilization of BNNTs. Dispersion was prepared with phosphate buffered solution (PBS). BNNTs (5 mg) were mixed with 10 mL of a 0.1% G-chitosan solution in a polystyrene tube. The samples were sonicated for 12 h (by a Bransonic sonicator 2510), using an output power of 20 W for all the experiments, resulting in a stable G-chitosan-BNNT dispersion by noncovalent coating of the nanotube walls with G-chitosan. The dispersion was characterized by spectrophotometric analysis, using a LIBRA S12 Spectrophotometer UV/vis/NIR (Biochrom). Microphotographs of the final dispersion of BNNTs were obtained with a FEI 200 FIB microscope and Zeiss 902 TEM, dropping a small quantity of BNNT aqueous suspension on a copper grid.

**Cell Culture, Viability Assay, and Up-Take Assessment.** The studies were performed on PC12 cells (ATCC CRL-1721), a cell line derived from a transplantable rat pheochromocytoma. PC12 cells respond reversibly to the administration of the nerve growth factor (NGF) by expressing the neuronal phenotype. As a matter of fact, NGF is responsible for phenotype commitment of PC12 cells toward sympathetic neurons. Additional salient effects of NGF in PC12 cell cultures include inhibition of proliferation, generation of long neurites, acquisition of electrical excitability, hypertrophy, and other changes associated with the acquisition of a neuronal-like phenotype.<sup>56</sup>

PC12 were cultured in Dulbecco's modified Eagle medium with 10% horse serum, 5% fetal bovine serum, 100 IU/mL penicillin, 100 µg/mL streptomycin, and 2 mM L-glutamine. Cells were maintained at 37 °C in a saturated humidity atmosphere (i.e., 95% air/5% CO<sub>2</sub>).

Additional experiments were carried out on human neuroblastoma SH-SY5Y cells (ATCC CRL-2266). This cell line represents a good model system for studying neuronal properties in culture, as many of their receptor systems have been well characterized and widely used as a model system for investigations in neurogenesis.<sup>57</sup> Treatment with retinoic acid has been reported to induce differentiation of SH-SY5Y cells, without altering the TrkA expression.<sup>58</sup> SH-SY5Y were cultured in Dulbecco's modified Eagle medium and Ham's F12 (1:1) with 10% fetal calf serum, 100 IU/mL penicillin, 100 µg/mL streptomycin, and 2 mM L-glutamine. Cells were maintained at 37 °C in a saturated humidity atmosphere containing 95% air/5% CO<sub>2</sub>. Compatibility of BNNTs on SH-SY5Y cells already has been widely documented.<sup>59</sup>

For viability testing, WST-1 (2-(4-iodophenyl)-3-(4-nitrophenyl)-5-(2,4-disulphophenyl)-2H-tetrazolium monosodium salt, provided in a premix electro-coupling solution, BioVision) cell proliferation assays were carried out. After trypsinization and counting with a hemocytometer, 5000 cells were seeded in 96-well plate chambers. Once adhesion was verified (after about 12 h since seeding), cells were incubated with 0, 5, 10, 20, 50, and 100 µg/mL of glycol-chitosan coated BNNTs for 3, 6, and 9 days. At the end point of incubation, cell cultures were treated with 100 µL of culture medium + 10 µL of the premix solution for a further 2 h and, thereafter, absorbance at 450 nm was read with a microplate reader (Victor3, Perkin-Elmer).

Viability was further investigated with the LIVE/DEAD viability/cytotoxicity kit (Molecular Probes). The kit contains calcein AM (4 mM in anhydrous DMSO) and ethidium homodimer-1 [EthD-1, 2 mM in DMSO/H<sub>2</sub>O 1:4 (v/v)]. After incubation for 72 h at GC-BNNT concentration of 10 µg/mL, the cells (25 000 in 24-well plate chambers, *n* = 3) were rinsed with PBS and treated for 10 min at 37 °C with 2 µM calcein AM and 4 µM EthD-1 in PBS. The cells were finally observed (after 9 days) using an inverted fluorescent microscope (TE2000U, Nikon) equipped with a cooled CCD camera (DS-5MC USB2, Nikon) and by NIS Elements imaging software, provided with the appropriate filters.

For early apoptosis detection, 25 000 cells were seeded in 24-well plate chambers (*n* = 3) and treated with 0–100 µg/mL of

glycol-chitosan coated BNNTs for 9 days. The ApoAlert kit (Clonetech Laboratories) was used to evaluate differences between normal and apoptotic cells after treatments. The kit contains annexin V-FITC (20 µg/mL in Tris-NaCl), 1X binding buffer, and propidium iodide (50 µg/mL in 1X binding buffer). The cells were rinsed with 1X binding buffer and then incubated with 200 µL of 1X binding buffer containing 5 µL of the annexin V solution and 10 µL of the propidium iodide solution. After incubation in the dark at room temperature for 20 min, the cells were observed via fluorescence microscopy with the appropriate filters.

Generation of reactive oxygen species (ROS) is a normal event for aerobic organisms, which occurs at a controlled rate in healthy cells. Under conditions of oxidative stress, like exposure to nanomaterials,<sup>60</sup> ROS production is dramatically increased, resulting in subsequent alteration of membrane lipids, proteins, and nucleic acids.

ROS production in PC12 cells treated with BNNTs was detected with use of the Image-IT Green Reactive Oxygen Species Detection kit (Invitrogen). The assay is based on 5-(and-6)-carboxy-2',7'-dichlorodihydrofluorescein diacetate (carboxy-H<sub>2</sub>DCFDA), a fluorogenic marker for ROS in viable cells. The non-fluorescent carboxy-H<sub>2</sub>DCFDA permeates live cells and is deacetylated by nonspecific intracellular esterases. In the presence of nonspecific ROS (produced throughout the cell, in particular during oxidative stress) the reduced fluorescein compound is oxidized and emits bright green fluorescence.<sup>61</sup> The cells (25 000 per well) were seeded in 24-well plate chambers (*n* = 3) and treated with 0–100 µg/mL of glycol-chitosan coated BNNTs for 9 days. They were then incubated for 45 min with a 25 µM carboxy-H<sub>2</sub>DCFDA working solution (in DMSO:PBS at 1:400 v/v) and immediately observed *via* fluorescence microscopy with the appropriate filters.

For both apoptosis and ROS detection, cell nuclei were counterstained with 5 µg/mL of Hoechst 33342.

Internalization was assessed by transmission electron microscopy (TEM). PC12 cells were seeded at  $2 \times 10^6$  cells/T25 flask. After attachment, they were incubated in a GC-BNNT modified CM (at a final concentration of 5 µg/mL). After 12 h of incubation, the samples were washed in PBS 0.1 M and then fixed when still adherent to flasks with 1% w/v glutaraldehyde–4% w/v paraformaldehyde in PBS 0.1 M pH 7.2 for 2 h at 4 °C. After washing, the cells were detached by scraping, postfixed in 1% w/v OsO<sub>4</sub> PBS 0.1 M pH 7.2 for 1 h, washed, and dehydrated with acidified acetone-dimethylacetate (Fluka) for 10 min. The samples were mixed in Epon/Durcupan resin in BEEM capsules #00 (Structure Probe) overnight at room temperature and finally embedded in resin at 56 °C for 48 h. Ultrathin sections (20–30 nm thick) were obtained with an Ultratome Nova ultramicrotome (LKB, Bromma, Sweden) equipped with a diamond knife (Diatome, Biel/Bienne, Switzerland).

The sections were placed on 200 square mesh nickel grids, counterstained with saturated aqueous uranyl acetate and lead citrate solutions, and observed with a Jeol JEM-2200FS microscope (Jeol, Japan). To assess the actual presence of BNNTs, B elemental map was obtained from the B K core-loss edge at 188 eV with the three windows method using a 20 eV energy slit. The EEL spectrum was acquired in STEM mode.

**Cell Stimulation Experiments.** PC12 cells were plated in 24-well chambers and kept in standard culture conditions for 24 h. Thus, CM was replaced with differentiating medium containing 2% fetal bovine serum, 100 IU/mL penicillin, 100 µg/mL streptomycin, 2 mM L-glutamine, and 60 ng/mL of NGF (N1418 from Sigma). Parallel experiments were carried out: cell cultured in differentiating medium with and without ultrasound (US) stimulation; cells cultured in BNNT-modified CM (5 and 10 µg/mL) with and without US stimulation, which was settled at 20 W, 40 kHz, for 5 s, 4 times a day for 9 days, performed with a Bransonic sonicator 2510.

For pharmacological inhibition of TrkA, cultures were treated with 200 nM K252a (Calbiochem) and monitored up to 6 days. Four parallel experiments were carried out: cells cultured in differentiating medium with and without ultrasound (US) stimulation; cells cultured in BNNT-modified CM (10 µg/mL) with and without US stimulation.

A number of experiments and analyses were carried out treating PC12 cells with  $\text{LaCl}_3$  (100  $\mu\text{M}$ ). In this case, lanthanum ions act as nonspecific calcium influx blockers, which allow the role of calcium ions to be investigated during the differentiation process.<sup>19</sup>

SH-SY5Y cells were plated in 24-well chambers and kept in standard culture conditions for 24 h. Thus, CM was replaced with differentiating medium containing 2% fetal bovine serum, 100 IU/mL penicillin, 100  $\mu\text{g/mL}$  streptomycin, 2 mM L-glutamine, and 10  $\mu\text{M}$  retinoic acid (R2625 from Sigma). Four parallel experiments were carried out: cells cultured in differentiating medium with and without ultrasound (US) stimulation; cells cultured in BNNT-modified CM (10  $\mu\text{g/mL}$ ) with and without US stimulation.

In all experiments the cells were stained with 2  $\mu\text{M}$  calcein AM for better visualization. Digital images were acquired and analyzed with ImageJ software for evaluation of differentiation, neurite length, and number of neurites per cell. More than 50 cells were analyzed for each experiment.

**Statistical Analysis.** Analysis of WST-1 data was performed by variance analysis (ANOVA) followed by the Student's *t*-test for significance, which was set at 5%. The analysis of differentiation data was performed following the Kruskal–Wallis procedure; *p*-values <0.05 were considered significant. WST-1 tests were performed in triplicate, the other experiments in triplicate. In all cases, three independent experiments were carried out. The results are presented as mean value  $\pm$  standard deviation.

**ACKNOWLEDGEMENTS** The authors would like to thank R. Brescia (Italian Institute of Technology) and C. Filippeschi (CRIM Lab) for TEM and FIB technical support, respectively.

## REFERENCES AND NOTES

- Gimsa, J.; Habel, B.; Schreiber, U.; van Rienen, U.; Strauss, U.; Gimsa, U. Choosing Electrodes for Deep Brain Stimulation Experiments - Electrochemical Considerations. *J. Neurosci. Methods* **2005**, *142*, 251–265.
- Adams, C.; Mathieson, K.; Gunning, D.; Cunningham, W.; Rahman, M.; Morrison, J. D.; Prydderch, M. L. Development of Flexible Arrays for in Vivo Neuronal Recording and Stimulation. *Nucl. Instrum. Methods Phys. Res., Sect. A* **2005**, *546*, 154–159.
- Valls-Solé, J.; Compta, Y.; Costa, J.; Valldeoriola, F.; Rumià, J. Human Central Nervous System Circuits Examined through the Electrodes Implanted for Deep Brain Stimulation. *Clin. Neurophysiol.* **2008**, *119*, 1219–1231.
- Albert, G. C.; Cook, C. M.; Prato, F. S.; Thomas, A. W. Deep Brain Stimulation, Vagal Nerve Stimulation and Transcranial Stimulation: An Overview of Stimulation Parameters and Neurotransmitter Release. *Neurosci. Biobehav. Rev.* **2009**, *33*, 1042–1060.
- Terrones, M.; Romo-Herrera, J. M.; Cruz-Silva, E.; López-Urías, F.; Muñoz-Sandoval, E.; Velázquez-Salazar, J. J.; Terrones, H.; Bando, Y.; Golberg, D. Pure and Doped Boron Nitride Nanotubes. *Mater. Today* **2007**, *10*, 30–38.
- Golberg, D.; Bando, Y.; Tang, C.; Zhi, C. Boron Nitride Nanotubes. *Adv. Mater.* **2007**, *19*, 2413–2432.
- Lacerda, L.; Bianco, A.; Prato, M.; Kostarelos, K. Carbon Nanotubes as Nanomedicines: From Toxicology to Pharmacology. *Adv. Drug Delivery Rev.* **2006**, *58*, 1460–1470.
- Ciofani, G.; Raffa, V.; Menciasci, A.; Cuschieri, A. Boron Nitride Nanotubes: An Innovative Tool for Nanomedicine. *Nano Today* **2009**, *4*, 8–10.
- Ciofani, G.; Raffa, V.; Menciasci, A.; Cuschieri, A. Cytocompatibility, Interactions and Uptake of Polyethyleneimine-Coated Boron Nitride Nanotubes by Living Cells: Confirmation of Their Potential for Biomedical Applications. *Biotechnol. Bioeng.* **2008**, *101*, 850–858.
- Ciofani, G.; Raffa, V.; Menciasci, A.; Cuschieri, A. Folate Functionalised Boron Nitride Nanotubes and their Selective Uptake by Glioblastoma Multiforme Cells: Implications for Their Use as Boron Carriers in Clinical Boron Neutron Capture Therapy. *Nanoscale Res. Lett.* **2009**, *4*, 113–121.
- Dai, Y.; Guo, E.; Zhang, Z.; Zhou, B.; Tang, C. Electric-Field-Induced Deformation in Boron Nitride Nanotubes. *J. Phys. D: Appl. Phys.* **2009**, *42*, 085403.
- Golberg, D.; Bai, X.; Mitome, M.; Tang, C.; Zhi, C.; Bando, Y. Structural peculiarities of in situ deformation of a multi-walled BN nanotube inside a high-resolution analytical transmission electron microscope. *Acta Mater.* **2007**, *55*, 1293–1298.
- Bai, X.; Golberg, D.; Bando, Y.; Zhi, C.; Tang, C.; Mitome, M. Deformation-Driven Electrical Transport of Individual Boron Nitride Nanotubes. *Nano Lett.* **2007**, *7*, 632–637.
- Martin, S. J.; Reutlingsperger, C. P.; McGahon, A. J.; Rader, J. A.; van Schie, R. C.; LaFace, D. M.; Green, D. R. Early Redistribution of Plasma Membrane Phosphatidylserine is a General Feature of Apoptosis Regardless of the Initiating Stimulus: Inhibition by Overexpression of Bcl-2 And Abl. *J. Exp. Med.* **1995**, *182*, 1545–1556.
- Yehia, H. N.; Draper, R. K.; Mikoryak, C.; Walker, E. K.; Bajaj, P.; Musselman, I. H.; Daigrepont, M. C.; Dieckmann, G. R.; Pantano, P. Single-Walled Carbon Nanotube Interactions with HeLa Cells. *J. Nanobiotechnol.* **2007**, *5*, 8.
- Raffa, V.; Ciofani, G.; Nitodas, S.; Karachalios, A. T.; D'Alessandro, D.; Masini, M.; Cuschieri, A. Can the Properties of Carbon Nanotubes Influence their Internalization by Living Cells. *Carbon* **2008**, *46*, 1600–1610.
- Tutak, W.; Park, K. H.; Vasilov, A.; Starovoytov, V.; Fanchini, G.; Cai, S. Q.; Partridge, N. C.; Sesti, F.; Chhowalla, M. Toxicity Induced Enhanced Extracellular Matrix Production in Osteoblastic Cells Cultured on Single-Walled Carbon Nanotube Networks. *Nanotechnology* **2009**, *20*, 255101.
- Luther, J. A.; Birren, S. J. p75 and TrkA Signaling Regulates Sympathetic Neuronal Firing Patterns via Differential Modulation of Voltage-Gated Currents. *J. Neurosci.* **2009**, *29*, 5411–5424.
- Kimura, K.; Yanagida, Y.; Haruyama, T.; Kobatake, E.; Aizawa, M. Electrically Induced Neurite Outgrowth of PC12 Cells on the Electrode Surface. *Med. Biol. Eng. Comput.* **1998**, *36*, 493–498.
- Manivannan, S.; Terakawa, S. Rapid Filopodial Sprouting Induced by Electrical Stimulation in Nerve Terminals. *Jpn. J. Physiol.* **1993**, *43*, 217–220.
- Ross, R. A.; Spengler, B. A.; Biedler, J. L. Coordinate morphological and biochemical interconversion of human neuroblastoma cells. *J. Natl. Cancer Inst.* **1983**, *71*, 741–747.
- Nicolini, G.; Miloso, M.; Zoia, C.; Di Silvestro, A.; Cavaletti, G.; Tredici, G. Retinoic Acid Differentiated SH-SY5Y Human Neuroblastoma Cells: An *in Vitro* model to Assess Drug Neurotoxicity. *Anticancer Res.* **1998**, *18*, 2477–2481.
- Olsson, A. K.; Vadhammar, K.; Nanberg, E. Activation and Protein Kinase C-Dependent Nuclear Accumulation of ERK in Differentiating Human Neuroblastoma Cells. *Exp. Cell Res.* **2000**, *256*, 454–467.
- Encinas, M.; Iglesias, M.; Llecha, N.; Comella, J. X. Extracellular-Regulated Kinases and Phosphatidylinositol 3-Kinase are Involved in Brain-Derived Neurotrophic Factor-Mediated Survival and Neuritegenesis of the Neuroblastoma Cell Line SH-SY5Y. *J. Neurochem.* **1999**, *73*, 1409–1421.
- McClellan, A. D.; Kovalenko, M. O.; Benes, J. A.; Schulz, D. J. Spinal Cord Injury Induces Changes in Electrophysiological Properties and Ion Channel Expression of Reticulospinal Neurons in Larval Lamprey. *J. Neurosci.* **2008**, *28*, 650–659.
- Udina, E.; Furey, M.; Busch, S.; Silver, J.; Gordon, T.; Fouad, K. Electrical Stimulation of Intact Peripheral Sensory Axons in Rats Promotes Outgrowth of Their Central Projections. *Exp. Neurol.* **2008**, *210*, 238–247.
- Wood, M.; Willits, R. K. Applied Electric Field Enhances DRG Neurite Growth: Influence of Stimulation Media, Surface Coating and Growth Supplements. *Bioelectromagnetics* **2006**, *27*, 328–331.
- Valentini, R. F.; Vargo, T. G.; Gardella, J. A., Jr.; Aebischer, P. Electrically Charged Polymeric Substrates Enhance Nerve Fibre Outgrowth *in Vitro*. *Biomaterials* **1992**, *13*, 183–190.

29. Gomez, N.; Schmidt, C. E. Nerve Growth Factor-Immobilized Polypyrrole: Bioactive Electrically Conducting Polymer for Enhanced Neurite Extension. *J. Biomed. Mater. Res., Part A* **2007**, *81*, 135–149.
30. Chew, S. Y.; Mi, R.; Hoke, A.; Leong, K. W. Aligned Protein-Polymer Composite Fibers Enhance Nerve Regeneration: A Potential Tissue-Engineering Platform. *Adv. Funct. Mater.* **2007**, *17*, 1288–1296.
31. Schmidt, C. E.; Shastri, V. R.; Vacanti, J. P.; Langer, R. Stimulation of Neurite Outgrowth Using an Electrically Conducting Polymer. *Proc. Natl. Acad. Sci. U.S.A.* **1997**, *94*, 8948–8953.
32. Valentini, R. F.; Vargo, T. G.; Gardella, J. A., Jr.; Aebischer, P. Patterned Neuronal Attachment and Outgrowth on Surface Modified, Electrically Charged Fluoropolymer Substrates. *J. Biomater. Sci., Polym. Ed.* **1993**, *5*, 13–36.
33. Aebischer, P.; Valentini, R. F.; Dario, P.; Domenici, C.; Galletti, P. M. Piezoelectric Guidance Channels Enhance Regeneration in The Mouse Sciatic Nerve after Axotomy. *Brain Res.* **1987**, *436*, 165–168.
34. Siskin, B. F.; Kanje, M.; Lundborg, G.; Herbst, E.; Kurtz, W. Stimulation of Rat Sciatic Nerve Regeneration with Pulsed Electromagnetic Fields. *Brain Res.* **1989**, *485*, 309–316.
35. Udina, E.; Furey, M.; Busch, S.; Silver, J.; Gordon, T.; Fouad, K. Electrical Stimulation of Intact Peripheral Sensory Axons in Rats Promotes Outgrowth of their Central Projections. *Exp. Neurol.* **2008**, *210*, 238–247.
36. Lyons, K. E.; Pahwa, R. Deep Brain Stimulation In Parkinson's Disease. *Curr. Neurol. Neurosci. Rep.* **2004**, *4*, 290–295.
37. Cellot, G.; Cilia, E.; Cipollone, S.; Rancic, V.; Sucupane, A.; Giordani, S.; Gambazzi, L.; Markram, H.; Grandolfo, M.; Scaini, D.; et al. Carbon Nanotubes Might Improve Neuronal Performance by Favouring Electrical Shortcuts. *Nat. Nanotechnol.* **2009**, *4*, 126–133.
38. Bekyarova, E.; Ni, Y.; Malarkey, E. B.; Montana, V.; McWilliams, J. L.; Haddon, R. C.; Parpura, V. Applications of Carbon Nanotubes in Biotechnology and Biomedicine. *J. Biomed. Nanotechnol.* **2005**, *1*, 3–17.
39. Gabay, T.; Jakobs, E.; Ben-Jacob, E.; Hanein, Y. Engineered Self-Organization of Neural Networks Using Carbon Nanotube Clusters. *Phys. A* **2005**, *350*, 611–621.
40. Gabay, T.; Ben-David, M.; Kalifa, I.; Sorkin, R.; Abrams, Z. R.; Ben-Jacob, E.; Hanein, Y. Electro-Chemical and Biological Properties of Carbon Nanotube Based Multi-Electrode Arrays. *Nanotechnology* **2007**, *18*, 35201.
41. Hu, H.; Ni, Y.; Montana, V.; Haddon, R. C.; Parpura, V. Chemically Functionalized Carbon Nanotubes as Substrates for Neuronal Growth. *Nano Lett.* **2004**, *4*, 507–511.
42. Lovat, V.; Pantarotto, D.; Lagostena, L.; Cacciari, B.; Grandolfo, M.; Righi, M.; Spalluto, G.; Prato, M.; Ballerini, L. Carbon Nanotube Substrates Boost Neuronal Electrical Signaling. *Nano Lett.* **2005**, *5*, 1107–1110.
43. Mattson, M. P.; Haddon, R. C.; Rao, A. M. Molecular Functionalization of Carbon Nanotubes and Use as Substrates for Neuronal Growth. *J. Mol. Neurosci.* **2000**, *14*, 175–182.
44. Mazzatenta, M.; Giugliano, S.; Campidelli, L.; Gambazzi, L.; Businaro, H.; Markram, M.; Prato, M.; Ballerini, L. Interfacing Neurons with Carbon Nanotubes: Electrical Signal Transfer and Synaptic Stimulation in Cultured Brain Circuits. *J. Neurosci.* **2007**, *27*, 6931–6936.
45. Sorkin, R.; Greenbaum, A.; David-Pur, M.; Anava, S.; Ayali, A.; Ben-Jacob, E.; Hanein, Y. Process Entanglement as a Neuronal Anchorage Mechanism to Rough Surfaces. *Nanotechnology* **2009**, *20*, 015101.
46. Zhang, X.; Prasad, S.; Niyogi, S.; Morgan, A.; Ozkan, M.; Ozkan, C. S. Guided Neurite Growth on Patterned Carbon Nanotubes. *Sens. Actuators, B* **2005**, *106*, 843–850.
47. Shein, M.; Greenbaum, A.; Gabay, T.; Sorkin, R.; David-Pur, M.; Ben-Jacob, E.; Hanein, Y. Engineered Neuronal Circuits Shaped and Interfaced with Carbon Nanotube Microelectrode Arrays. *Biomed. Microdevices* **2009**, *11*, 495–501.
48. Keefer, E. W.; Botterman, B. R.; Romero, M. I.; Rossi, A. F.; Gross, G. W. Carbon Nanotube Coating Improves Neuronal Recordings. *Nat. Nanotechnol.* **2008**, *3*, 434–439.
49. Matsumoto, K.; Sato, C.; Naka, Y.; Whitby, R.; Shimizu, N. Stimulation of Neuronal Neurite Outgrowth Using Functionalized Carbon Nanotubes. *Nanotechnology* **2010**, *21*, 115101.
50. Della Flora, E.; Perera, C. L.; Cameron, A. L.; Maddern, G. J. Deep Brain Stimulation for Essential Tremor: A systematic review. *Movement Disord.* **2010**, *25*, 1550–1559.
51. Xu, J.; Chen, J. D. Z. Intestinal Electrical Stimulation Improves Delayed Gastric Emptying and Vomiting Induced by Duodenal Distension in Dogs. *Neurogastroenterol. Motil.* **2008**, *20*, 236–242.
52. Ross, K. B.; Dubin, S.; Nigroni, P.; Kepics, F.; Shi, W. Y.; Yan, H. Programmed Stimulation for Simulation of Atrial Tachyarrhythmias. *Biomed. Sci. Instrum.* **1997**, *33*, 25–29.
53. Gordon, T.; Brushart, T. M.; Amirjani, N.; Chan, K. M. The Potential of Electrical Stimulation to Promote Functional Recovery after Peripheral Nerve Injury — Comparisons between Rats and Humans. *Acta Neurochir.* **2007**, *100*, 3–11.
54. Ciofani, G. Potential Applications of Boron Nitride Nanotubes as Drug Delivery Systems. *Expert Opin. Drug Delivery* **2010**, *7*, 889–893.
55. <http://ncm.wit.edu.cn/english.jsp>.
56. Greene, L. A.; Farinelli, S. E.; Cunningham, M. E.; Park, D. S. Methodologies for the Culture and Experimental Use of the PC12 Rat Pheochromocytoma Cell Line. In *Culturing Nerve Cells*; Banker, F., Goslin, K., Eds.; MIT Press: Cambridge, MA, 1998; Vol. 2.
57. Kaplan, D. R.; Matsumoto, K.; Lucarelli, E.; Theile, C. J. Induction of TrkB by Retinoic Acid Mediates Biologic Responsiveness to BDNF and Differentiation of Human Neuroblastoma Cells. *Neuron* **1993**, *11*, 321–331.
58. Encinas, M.; Iglesias, M.; Llechas, N.; Comella, J. X. Extracellular-Regulated Kinases and Phosphatidylinositol 3-Kinase Are Involved in Brain-Derived Neurotrophic Factor-Mediated Survival and Neuritegenesis of the Neuroblastoma Cell Line SH-SY5Y. *J. Neurochem.* **1999**, *73*, 1409–1421.
59. Ciofani, G.; Danti, S.; D'Alessandro, D.; Moscato, S.; Mencias, A. Assessing Cytotoxicity of Boron Nitride Nanotubes: Interference with the MTT Assay. *Biochem. Biophys. Res. Commun.* **2010**, *394*, 405–411.
60. Pulskamp, K.; Diabatè, S.; Krug, H. F. Carbon Nanotubes Show no Sign of Acute Toxicity but Induce Intracellular Reactive Oxygen Species in Dependence on Contaminants. *Toxicol. Lett.* **2007**, *168*, 58–74.
61. Park, E. J.; Choi, J.; Park, Y. K.; Park, K. Oxidative Stress Induced by Cerium Oxide Nanoparticles in Cultured BEAS-2B Cells. *Toxicology* **2008**, *245*, 90–100.